Kinetic phase transition in $A_2+B_2\rightarrow 2AB$ reaction system

Da-yin Hua,* Shi-jie Shao, and Su Lin
Physics Department, Laboratory of Nano-materials and Technology, Ningbo University, Ningbo 315211, People's Republic of China
(Received 14 October 2003; published 28 April 2004)

Three lattice gas models for $A_2+B_2\rightarrow 2AB$ reaction system are studied by Monte Carlo simulation in two-dimensional triangular lattice surface. When both A_2 and B_2 adsorb and dissociate on the catalytic surface in the random dimer-filling mechanism or in the end-on dimer-filling mechanism, there is no reactive window in the reaction system and just a discontinuous phase transition appears from a "B+vacancy" poisoned state to an "A+vacancy" poisoned state. However, a reactive window appears when one of the two dimers, A_2, dissociates in the random dimer-filling mechanism but another dimer, B_2, is in the end-on dimer-filling mechanism and the system exhibits a discontinuous phase transition from the active reaction state to a B+vacancy poisoned state and a continuous phase transition to an "A+vacancy" poisoned state. Furthermore, we show that the critical behavior of the continuous phase transition with infinitely many absorbing states belongs to the robust directed percolation universality class.

DOI: 10.1103/PhysRevE.69.046114 PACS number(s): 05.70.Ln

Recently, the nonequilibrium dynamical phase transition exhibiting in numerous lattice gas models about the surface catalytic reaction has received widespread attention since Ziff, Gulari, and Barshed introduced a most popular model to describe the catalytic oxidation of the CO [1–3]. In that model, a gas composed of CO and O_2 molecules with a fixed fraction y_{co} and $1-y_{\mathrm{co}}$, respectively, is allowed to contract with a square lattice surface. A CO molecule can occupy a vacant site, while O_2 molecule can dissociate and fill each site of any nearest-neighbor (NN) pair of vacancies. Adsorbed CO and O atoms at nearest-neighbor sites can react immediately to form CO_2 which leaves the surface at once. This model is shown to exhibit two phase transitions between active and poisoned states: for $y_{\mathrm{co}}<y_1$, an O-poisoned system is formed, while for $y_{\mathrm{co}}>y_2$ the reaction system is poisoned by CO. For $y_1<y_{\mathrm{co}}<y_2$ the reaction on the surface can continue. At y_1 the phase transition is continuous, whereas at y_2 the transition is discontinuous.

Heterogeneous catalytic reactions are very complicated and very difficult to deal with from experiment or from theory, therefore, the study of many computer models is very important and obtains many results [3–9]. In many previous lattice model investigations, a pair of NN sites for the dimer adsorbing trial is randomly selected in the simulation process, which we characterize as the random dimer-filling mechanism [3,7,8,10,11]. Therefore, the configuration of the adsorbate on surface does not affect the selection of a pair for the dimer adsorption. However, for an actual reaction on surface, the adsorbing process of the dimer involves a very complicated dissociation on surface, and its dissociation depends on the surrounding chemical environment. Moiny and co-workers have shown that the intrinsic adsorbate cluster on the heterogeneous catalytic reaction surface has an important effect on the reaction kinetics [12–14]. On the other hand, Evans and co-workers [11,15,16] and Hua and Ma [17] have shown that a variation of the random dimer-filling mechanism, which is called "end-on dimer-filling" mechanism, can have an important influence on the monomer-dimer model.

In the present paper, we investigate three lattice gas models for $A_2+B_2\rightarrow 2AB$ reaction system considering different dimer dissociation processes with a triangular lattice in two-dimensional surface. When both A_2 and B_2 adsorb and dissociate in the random dimer-filling mechanism or in the end-on dimer-filling mechanism, there is no reactive window in the reaction system and just a discontinuous phase transition appears from a "B+vacancy" poisoned state to an "A+vacancy" poisoned state. However, it is found that a reactive window appears when dimer A_2 dissociates in the random dimer-filling mechanism but dimer B_2 dissociates in the end-on dimer-filling mechanism, and that the system exhibits a discontinuous phase transition from the active reaction state to a B+vacancy poisoned state and a continuous phase transition to an A+vacancy poisoned state. Furthermore, we show that the critical behavior of the continuous phase transition in the system is in the robust directed percoation (DP) universality class.

We model our catalytic surface by a triangular lattice, which is in contrast with an infinite reservoir of the two types of dimers, labeled here by A_2 and B_2. These dimers can be adsorbed onto the lattice and dissociate into two atoms, which occupy two nearest-neighbor sites of the lattice, and they can react according to the following steps: (1) $A_{2(g)}+2v\rightarrow 2A_{(ads)}$, (2) $B_{2(g)}+2v\rightarrow 2B_{(ads)}$, and (3) $A_{(ads)}+B_{(ads)}\rightarrow AB_{(g)}+2v$, in which the subscript (g) denotes the species in the gas phase and (ads) means that the species is adsorbed on the lattice surface. Here v indicates a vacant site on the lattice.

In our system, the dissociation of dimer can follow one of the two mechanisms, which are random and end-on dimer-filling mechanisms. For the random dimer-filling mechanism, first randomly pick one site (if empty), then randomly select a NN site from the six NN sites, the dimer fills only if both sites are empty. As a result, a pair of NN sites is selected randomly for the dimer adsorption.

The end-on filling mechanism: randomly pick one site i, and if i and at least one of the six NN sites are empty, then

*Author to whom correspondence should be addressed.

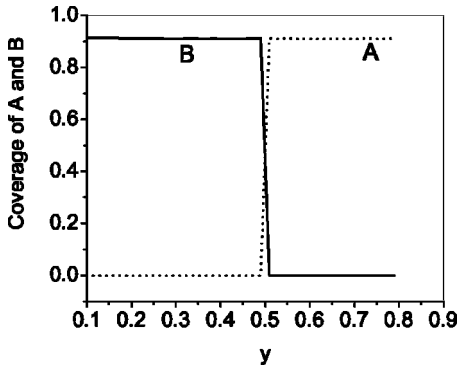

FIG. 1. The stationary state phase diagram for model (i). The average coverage of A and B is plotted as a fraction of y. Phase transition occurs at $y=0.5$.

occupy i and an empty site selected randomly from the empty NN site. Obviously, whether the NN site is occupied or not should have a different effect on the dissociation of the adsorbed dimer. Therefore, the selection of a pair for the dimer adsorbing trial is no longer purely random because the configuration of the adsorbate on the catalytic surface significantly affects the selection.

In our simulation, we include three cases. Model (i): both dimers A_2 and B_2 dissociate in the random dimer-filling mechanism. Model (ii): B_2 dissociates in the end-on mechanism but A_2 is in the random dimer-filling mechanism. Model (iii): both A_2 and B_2 dissociate in the end-on filling mechanism.

If a dimer adsorbs successfully, the two adsorbed atoms react with another different kind of atom selected randomly on the NN sites to produce an AB molecule immediately which desorbs at once and leaves two vacant sites.

A simulation begins with a collision of a dimer A_2 (or B_2) with a probability y (or $1-y$) which is the fraction of A_2 in gas phase on a $L\times L$ triangular lattice with an initial empty lattice and periodic boundary conditions.

For model (i), the phase diagram is shown in Fig. 1. The reaction system exhibits a discontinuous phase transition at $y=0.5$ from a B+vacancy poisoned state to an A+vacancy poisoned state with the increasing fraction of y. It is obvious that there is no reaction window as the reaction system follows the model (i) mechanism and the simulation result is consistent with the previous works [18,19].

When the reaction system satisfies the mechanism in the model (ii), the phase diagram is shown in Fig. 2. Compared to Fig. 1, it is found that a reaction window appears in Fig. 2. Furthermore, with varying y, the system exhibits a discontinuous phase transition at $y=0.62\pm0.01$ from the reactive state to a B+vacancy poisoned state and a continuous transition to an A+vacancy poisoned state.

However, when the reaction system satisfies the model (iii), both the reaction dimers dissociate in the end-on filling mechanism, the reaction window disappears as shown in Fig. 3 and just a discontinuous transition is exhibited at $y=0.5$ with increasing y as in Fig. 1.

In Fig. 2, there are infinitely many absorbing states (i.e., from which the system cannot escape) for the continuous phase transition and it is very interesting about the critical

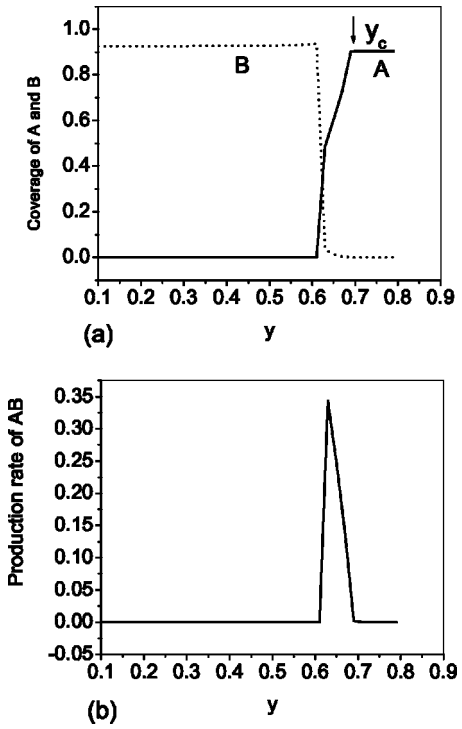

FIG. 2. The stationary state phase diagram for model (ii) showing three areas. The coverage of A, B, and the production rate of AB are plotted as a fraction of y.

behavior [1,2]. It is quite difficult to directly estimate the accurate critical point value y_c and corresponding critical behaviors at y_c[20] due to the critical slowing down and strong finite-size effects. In this work, we employ the finite-size scaling (FSS) method developed for the nonequilibrium continuous phase transition by Aukrust, Browne, and Webman [17,20,21] to estimate the critical point y_c, the order parameter exponent β, and other correlation length exponents.

The order parameter describing the absorbing phase transition is ρ, $\rho=\rho_A^{sat}-\rho_A$, in which ρ_A^{sat} is the average saturated coverage of A on the surface and ρ_A is the coverage of A. The order parameter ρ behaves as below when y is in the neighborhood of the critical point y_c,

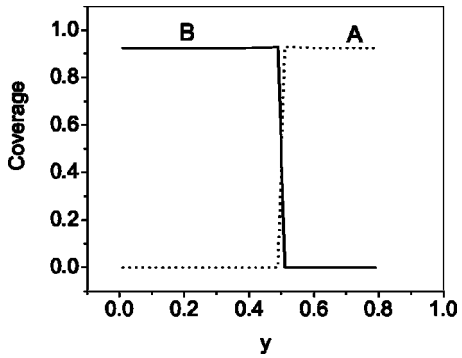

FIG. 3. The stationary state phase diagram for model (iii). The average coverage of A and B is plotted as a fraction of y. Phase transition occurs at $y=0.5$.

$$\rho \propto (y_c - y)^{\beta}, \tag{1}$$

where β is the order parameter exponent, and the critical point y_c is accurately estimated by the FSS method. When y is near to the critical point y_c of the second-order phase transition, there are a characteristic length scale ξ and a time scale τ which denote the correlation length in space and time direction, respectively, and they diverge in the neighborhood of the critical point as

$$\xi \propto |y_c - y|^{-\upsilon_\perp}, \tag{2}$$

$$\tau \propto |y_c - y|^{-\upsilon_\parallel}, \tag{3}$$

where $\upsilon_\perp(\upsilon_\parallel)$ is a correlation length exponent in the space (time) direction.

At critical point, various ensemble-averaged quantities depend on the system size L through the ratio of the system size and the correlation length L/ξ, therefore, the order parameter $\rho(y,L)$ satisfies the following scaling form in the neighborhood of the critical point:

$$\rho(y,L) \propto L^{-\beta/\upsilon_\perp} f[(y_c - y)L^{1/\upsilon_\perp}], \tag{4}$$

so that at y_c,

$$\rho(y_c,L) \propto L^{-\beta/\upsilon_\perp}, \tag{5}$$

and the scaling function

$$f(x) \propto x^{\beta} \tag{6}$$

for large x. In the supercritical region $(y<y_c)$, the order parameter $\rho(y,L)$ remains finite in the limit $L\rightarrow\infty$, but it decays faster than a power law in the subcritical region $(y>y_c)$.

For the characteristic time τ, we can take the following finite-size scaling form in the vicinity of y_c:

$$\tau(y,L) \propto L^z h[(y_c - y)L^{1/\upsilon_\perp}], \tag{7}$$

where $z=\upsilon_\parallel/\upsilon_\perp$ is the usual dynamical exponent. At y_c we have

$$\tau(y_c,L) \propto L^z. \tag{8}$$

We calculate the moments τ_s for each sample s which denotes a simulation entering the absorbing state from the initial empty state, therefore, we can measure the characteristic time τ following the equation:

$$\tau_s(y,L,s) = \sum_t t\rho(y,L,t,s) / \sum_t \rho(y,L,t,s), \tag{9}$$

where $\tau=\langle\tau_s\rangle_s$, and $\rho(y,L,t,s)$ is the order parameter defined above.

The system first reaches a quasisteady state, stays for a reasonably long time, and finally evolves into an absorbing state. In the simulation process, we first calculate the average saturated coverage of A as ρ_A^{sat} over a large number of samples which enters into a poisoned state, then calculate an average of time series of the difference $(\rho_A^{sat}-\rho_A)$ (ρ_A is coverage of A as mentioned above) over a set of surviving independent samples which have not yet entered the absorbing state when the simulation ends, then measure the stationary state value of the time series as order parameter from the average of time series. The number of Monte Carlo steps varies from 100 for $L=8$ to 4×10^3 for $L=128$ (a Monte Carlo step refers to an attempted adsorption-reaction step on the average at every lattice site). From about 10 000 independent simulations, we choose 2000 surviving samples to calculate the order parameter ρ when $L=8$. The number of independent surviving samples varies from 2000 for $L=8$ to 400 for $L=128$.

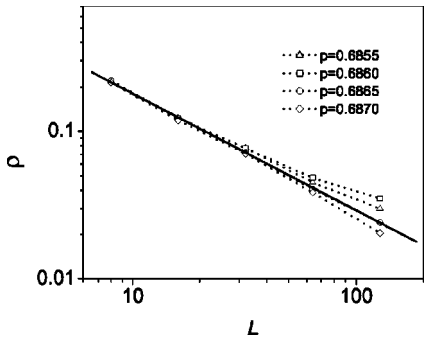

FIG. 4. The log-log plot for $\rho(y,L)$ vs L with different values of y for model (ii). The slope of the straight line that goes through the data gives an estimate of $-\beta/\upsilon_\perp$.

From Eq. (5), the data should fall on a straight line with a slope $-\beta/\upsilon_\perp$ for $y=y_c$ on a log-log plot of ρ as a function of L. In Fig. 4, we show the log-log plot of ρ as a function of L when $L=8,16,32,64$, and 128. For our system, we find $y_c=0.6865\pm0.0005$, and $\beta/\upsilon_\perp=0.80\pm0.01$ at y_c from the slope of the straight line. This value of $\beta/\upsilon_\perp$ is in excellent agreement with that (0.80 ± 0.01) of the DP universality class [28], in contrast to the earlier result. We can get further supporting results.

In Fig. 5, we have plotted $\rho L^{\beta/\upsilon_\perp}$ versus $(1-y/y_c)L^{1/\upsilon_\perp}$ on a double-logarithmic plot. From Eqs. (4) and (6), when x is small, the data should approach a constant, while for large x, the data should fall on a line with a slope β. It is shown that with the choices $\beta/\upsilon_\perp=0.80$ and $\upsilon_\perp=0.73$, the data for the various system sizes are well collapsed on a single curve. The solid line has a slope of 0.58 ± 0.02, which gives the asymptotic behavior for $\rho L^{\beta/\upsilon_\perp}$ as $L\rightarrow\infty$.

We can also calculate the decay exponent of the order parameter at the critical point. For the time dependence of

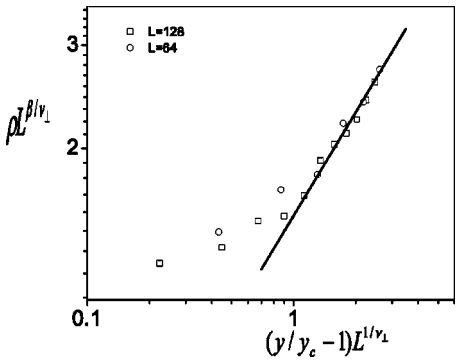

FIG. 5. The double-logarithmic plot for the data of $\rho L^{\beta/\upsilon_\perp}$ against $(1-y/y_c)L^{1/\upsilon_\perp}$ for various system sizes.

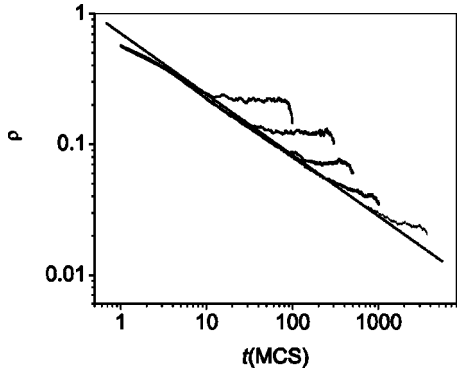

FIG. 6. The time dependence of the order parameter ρ for various size L at $y_c=0.6865$. From top to bottom, the curves correspond to $L=8,16,32,64$, and 128. The slope of the straight line gives the value of $\beta/\nu_{\|}(=0.45\pm0.01)$.

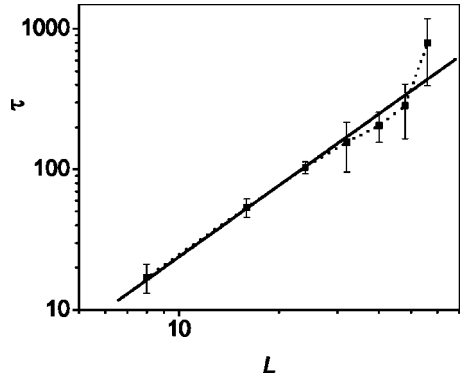

FIG. 7. The characteristic time τ against the system size L in log-log plot. The solid line is of slope $1.69(=\nu_{\|}/\nu_{\perp})$.

the order parameter $\rho(y_c,L,t)$ at criticality, one assumes a scaling form

$$\rho(y_c,L,t) \propto L^{-\beta/\nu_{\perp}} f(tL^{-\nu_{\|}/\nu_{\perp}}). \tag{10}$$

For $L \gg 1$ and $t \ll L^{\nu_{\|}/\nu_{\perp}}$, we have the relation $\rho(y_c,L,t) \propto t^{-\beta/\nu_{\|}}$. In Fig. 6, we show the double-logarithmic plot of $\rho(t)$ as a function of time t, and then we get $\beta/\nu_{\|} = 0.45\pm0.01$, which is consistent with the above results. Moreover, in Fig. 7, we show the characteristic time τ as a function of L on a log-log plot. From Eq. (8), the data should fall on a line with the slope $z=\nu_{\|}/\nu_{\perp}$ at the critical point. Every calculation result is averaged over 10 000 samples, and we obtain the slope $z=1.69\pm0.15$ at $y_c = 0.6865$.

From the above simulation results, $\beta/\nu_{\perp}=0.80\pm0.01$, $\beta = 0.58\pm0.02$, $\beta/\nu_{\|}=0.45\pm0.01$, $z=1.69\pm0.15$, it is shown that the critical behavior of the continuous transition with infinitely-many absorbing states in the model (ii) belongs to the robust DP universality class [22–28].

In conclusion, we investigate three lattice gas models for $A_2+B_2\rightarrow 2AB$ reaction system under different dimer dissociation processes with a triangular lattice in two-dimensional surface. When both A_2 and B_2 dissociate in the random dimer-filling mechanism or in the end-on dimer-filling mechanism, there is no reactive window in the reaction system and just a discontinuous phase transition appears from a B+vacancy poisoned state to an A+vacancy poisoned state. However, it is found that a reactive window appears when one of the two dimers, A_2, dissociates in the random dimer-filling mechanism but another dimer, B_2, is in the end-on dimer filling and that the system exhibits a discontinuous phase transition from an active reaction state to a B +vacancy poisoned state and a continuous phase transition to an A+vacancy poisoned state. Furthermore, we show that the critical behavior of the continuous phase transition with infinitely many absorbing states is in the robust DP universality class. On the other hand, the particle diffusion is neglected in our three models, however, it will have an important effect on the phase transition and the critical behavior in the model (ii), we will report the investigation results elsewhere. We believe that further understanding will be highly desirable.

This work was supported by Ningbo Youth Foundation (Grant No. 2003A62007).

[1] J. Marro and R. Dickman, *Non-Equilibrium Phase Transitions in Lattice Models* (Cambridge University Press, Cambridge, England, 1999).
[2] H. Hinrichsen, Adv. Phys. **49**, 815 (2000).
[3] R. M. Ziff, E. Gulari, and Y. Barshad, Phys. Rev. Lett. **56**, 2553 (1986).
[4] V. P. Zhdanov, Surf. Sci. Rep. **45**, 231 (2002).
[5] J. W. Evans, Langmuir **7**, 2514 (1991).
[6] O. Kortluke and W. von Niessen, J. Chem. Phys. **105**, 4764 (1996).
[7] V. P. Zhdanov, J. Chem. Phys. **110**, 8748 (1999); Phys. Rev. E **59**, 6292 (1999).
[8] M. A. Khan, K. Yaldram, G. K. Khalil, and K. M. Khan, Phys. Rev. E **50**, 2156 (1994).
[9] Da-yin Hua and Yu-qiang Ma, Phys. Rev. E **64**, 056102 (2001); **66**, 066103 (2002); **67**, 056107 (2003).
[10] I. Jensen, H. C. Fogedby, and R. Dickman, Phys. Rev. A **41**, 3411 (1990).
[11] R. S. Nord and J. W. Evans, J. Chem. Phys. **93**, 8397 (1990).
[12] F. Moiny and M. Dumont, J. Chem. Phys. **115**, 7705 (2001).
[13] F. Moiny, M. Dumont, and R. Dagonnier, J. Chem. Phys. **108**, 4572 (1998).
[14] F. Moiny and M. Dumont, J. Chem. Phys. **111**, 4743 (1999).
[15] M. Tammaro and J. W. Evans, Phys. Rev. E **52**, 2310 (1995).
[16] J. W. Evans and R. S. Nord, Phys. Rev. B **31**, 1759 (1985).
[17] Da-yin Hua and Yu-qiang Ma, Phys. Rev. E **66**, 036101 (2002).
[18] K. M. Khan, K. Yaldram, N. Ahmad, and Qamar -ul-Haque, Physica A **268**, 89 (1999).
[19] Xiao Han and Z. R. Yang, Physica A **307**, 41 (2002).

[20] T. Aukrust, D. Browne, and I. Webman, Phys. Rev. A **41**, 5294 (1990).
[21] M. H. Kim and H. Park, Phys. Rev. Lett. **73**, 2579 (1994); Phys. Rev. E **52**, 5664 (1995).
[22] H. K. Janssen, Z. Phys. B: Condens. Matter **42**, 151 (1981).
[23] P. Grassberger, Z. Phys. B: Condens. Matter **47**, 365 (1982).
[24] G. Grinstein, Z. W. Lai, and D. A. Brown, Phys. Rev. A **40**, 4820 (1989).
[25] I. Jensen and R. Dickman, Phys. Rev. E **48**, 1710 (1993).
[26] I. Jensen, Phys. Rev. E **47**, R1 (1993).
[27] H. Takayasu and A. Yu. Tretyakov, Phys. Rev. Lett. **68**, 3060 (1992).
[28] M. A. Munoz, R. Dickman, A. Vespignani, and S. Zapperi, Phys. Rev. E **59**, 6175 (1999).